Developmental Cell
Article

Mammalian SEPT2 Is Required for Scaffolding Nonmuscle Myosin II and Its Kinases

Emily Joo,[1] Mark C. Surka,[1,2] and William S. Trimble[1,*]
[1]Program in Cell Biology, Hospital for Sick Children, Department of Biochemistry, University of Toronto, Toronto, Ontario M5G 1X8, Canada
[2]Present address: The Scripps Research Institute, Department of Cell Biology, 10550 North Torrey Pines Road, La Jolla, CA 92037, USA.
*Correspondence: wtrimble@sickkids.ca
DOI 10.1016/j.devcel.2007.09.001

SUMMARY

Mammalian septin SEPT2 belongs to a conserved family of filamentous GTPases that are associated with actin stress fibers in interphase cells and the contractile ring in dividing cells. Although SEPT2 is essential for cytokinesis, its role in this process remains undefined. Here, we report that SEPT2 directly binds nonmuscle myosin II (myosin II), and this association is important for fully activating myosin II in interphase and dividing cells. Inhibition of the SEPT2-myosin II interaction in interphase cells results in loss of stress fibers, while in dividing cells this causes instability of the ingressed cleavage furrow and dissociation of the myosin II from the Rho-activated myosin kinases ROCK and citron kinase. We propose that SEPT2-containing filaments provide a molecular platform for myosin II and its kinases to ensure the full activation of myosin II that is necessary for the final stages of cytokinesis.

INTRODUCTION

Properly regulated cell division is necessary for the development and survival of all multicellular organisms. In fact, it was reported that the inhibition of cytokinesis in p53 null cells led to genomic instability and tumorigenesis (Fujiwara et al., 2005), supporting the contention that abnormal cytokinesis can lead to cancer. Most mammalian cells achieve cell division by constructing a cleavage furrow where ingression is accomplished through the contractile action of nonmuscle myosin (myosin II) on actin filaments (Glotzer, 2001). Actomyosin-mediated cytokinesis can be divided arbitrarily into four different stages. The first stage involves selection of the cleavage plane and recruitment of the actomyosin ring and associated components. Actin and myosin, major components of stress fibers, disassemble during interphase and relocalize to the nascent cleavage furrow. In the second stage, cleavage furrow ingression is initiated through the contractile activity of myosin. The hetero-hexameric myosin II protein complex forms filaments that bind to actin fibers. Next, the intercellular bridge (midbody) is stabilized, and finally, the abscission of the midbody is achieved (Glotzer, 2001).

It is believed that the phosphorylation of the regulatory myosin light chain at residues 18 and 19 (pMLC-S19 and ppMLC-S19T18) determines the ability of the myosin II heavy chain to bind to and move along actin filaments (Sellers, 1999). Interestingly, while mono-phosphorylation can activate the ATPase activity and support actin motility in vitro, di-phosphorylation results in 2-fold higher ATPase activity, thick actin filament assembly (Ikebe and Hartshorne, 1985), and enhanced tension in stress fibers (Mizutani et al., 2006), suggesting a possible role in actin bundling. Moreover, di-phosphorylation is highly enriched at the cleavage furrow of dividing cells (Yamashiro et al., 2003) along with a number of other proteins including the septins.

Septins are a family of filamentous GTPases identified more than 30 years ago in a screen for genes important for cell division in budding yeast (Hartwell, 1971), and subsequent studies identified septins in other species. In most instances, the role of septin in cell division seems to be conserved. However in *S. pombe*, mutations in septins only delayed cytokinesis (Berlin et al., 2003; Tasto et al., 2003), in *C. elegans* they are only required for some cell divisions (Nguyen et al., 2000), and some mammalian septins are only found in nondividing cells such as neurons (Xue et al., 2004) suggesting that the role of septins is not confined to cytokinesis. In yeast, septins have been proposed to act as scaffolds for signaling components (Hanrahan and Snyder, 2003), diffusion barriers (Barral et al., 2000; Takizawa et al., 2000), guides for orienting the spindle pole body (Kusch et al., 2002), and cell cycle checkpoints (Castillon et al., 2003). To date, 14 different mammalian septin genes have been described. These mammalian septins have been linked to a variety of processes including the establishment of cell polarity, cellular morphogenesis, membrane fusion, and neoplasia (Joo et al., 2005), yet how they are contributing to these different processes is not clear.

Mammalian septins, similar to yeast septins, coisolate together in complexes (e.g., SEPT6, SEPT7, and SEPT9 are copurified with SEPT2), and these protein complexes are posited to be a core unit for the generation of the septin filaments (Kinoshita et al., 2002; Sheffield et al.,

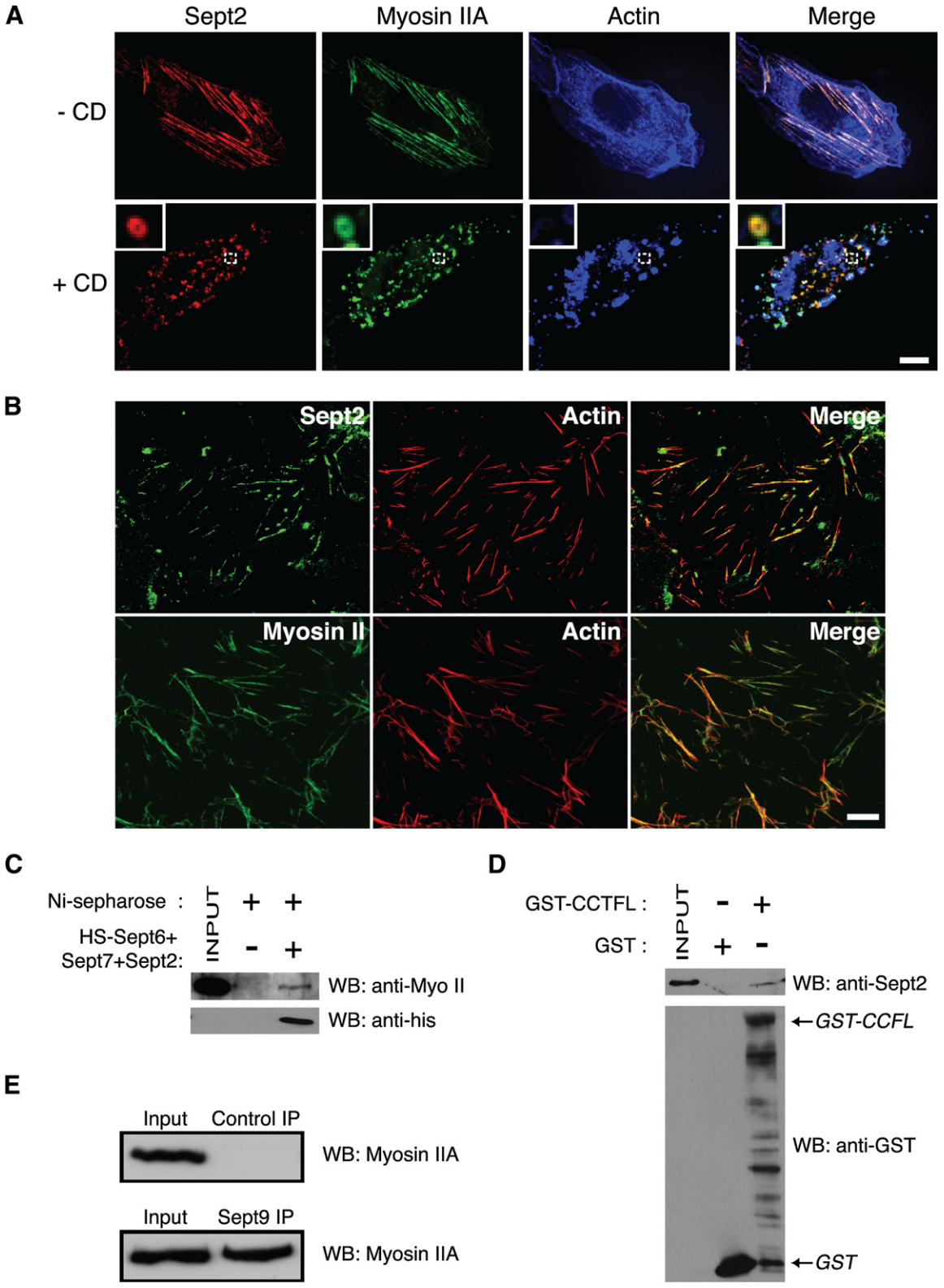

Figure 1. SEPT2 Associates with Myosin II

(A) Confocal images of CHO-K1 cells transfected with GFP-myosin IIA (green) and treated with or without 3 μM cytochalasin D (CD). Endogenous SEPT2 and F-actin were visualized by immunostaining with anti-SEPT2 antibody (red) and staining with Alexa 633-phalloidin (blue), respectively. In the bottom row, a representative ring (hatched box) is shown in inset.

2003; Versele et al., 2004). SEPT2 and SEPT9 have been shown to be required for cytokinesis as microinjection of inhibitory antibodies or depletion of these proteins using siRNA resulted in a failure of cytokinesis and a subsequent increase in binucleated cells (Kinoshita et al., 1997; Surka et al., 2002). Mammalian septin-associated proteins include syntaxins (Beites et al., 1999), borgs (Joberty et al., 2001), and anillin (Kinoshita et al., 2002). It has been suggested that septins associate with the plasma membrane through syntaxins or anillin, although they are also known to directly interact with phospholipids (Zhang et al., 1999).

Here, we investigate the role of SEPT2 in the organization of contractile actin filaments and identify a binding partner, nonmuscle myosin II. Nonmuscle myosin II isoform A (hereafter referred to as myosin II) binds directly to SEPT2 and acts as an adaptor protein linking SEPT2 to the actin filaments. Moreover, a significant decrease in the di-phosphorylated myosin light chain (ppMLC-S19T18) was observed when SEPT2 is dissociated from myosin II, suggesting that SEPT2 or SEPT2-containing septin filaments act as a scaffold, holding myosin II and myosin kinases in close proximity to ensure maximal myosin activation for certain contractile processes. We propose that this septin scaffold is essential for a proper spatiotemporal regulation of myosin II during the late stages of cytokinesis.

RESULTS

Septin 2 Associates with Nonmuscle Myosin II

Septin 2 (SEPT2) is known to colocalize with contractile actin stress fibers (Kinoshita et al., 1997), but forms ring structures of approximately 500 nm in diameter when the actin stress fibers are disassembled by cytochalasin D (Kinoshita et al., 2002). As expected, we found that SEPT2 colocalized with myosin II, a component of contractile filaments, in untreated cells; however, to our surprise, this SEPT2-myosin II association was maintained in the absence of the actin filaments (Figure 1A). GFP-tagged myosin II isoform A and B formed rings that colocalized with SEPT2 rings (insets of Figure 1A; data not shown). Anillin, a protein proposed to serve as an adaptor between septins and actin during mitosis (Kinoshita et al., 2002), was not detected with these rings even when immunostaining was performed with a very high concentration of anti-anillin antibody (data not shown). This is consistent with the observation that anillin normally resides in the nucleus and becomes cytoplasmic only when the nuclear envelope breaks down during cell division (Oegema et al., 2000).

Four different methods were used to confirm this novel interaction between SEPT2 and myosin II. The first approach involved isolation of stress fibers from CHO-K1 cells adhered to glass coverslips (Katoh et al., 1998). This isolation was achieved by a lysis system that consists of a low-ionic-buffer extraction followed by two short detergent extractions (Katoh et al., 1998). Under these conditions, in which most of the cytosolic, membrane, or cell cortex-associated proteins are washed away, leaving behind only a number of actin stress fiber-associated proteins (Katoh et al., 1998), SEPT2 and myosin II were each clearly coextracted with actin stress fibers (Figure 1B). The second approach involved pull-down of native myosin II protein from CHO cell lysate using recombinant SEPT2, SEPT6, and SEPT7 (SEPT2/6/7) subcomplexes (Sheffield et al., 2003) that are immobilized on Ni-sepharose beads. Native myosin II proteins were selectively pulled down with the Ni-sepharose beads decorated with septin subcomplexes but not the beads alone (Figure 1C). The third approach involved the reciprocal pull-down of native SEPT2 protein using a recombinant fragment of myosin IIA. The latter half of the myosin IIA protein or CCFL (Figure 2B) expressed as a GST-fusion protein was immobilized on glutathione beads and, despite the extensive degradation of this large fusion protein during its purification, native SEPT2 was copurified only with the glutathione beads decorated with myosin IIA fragment (Figure 1D). The fourth approach involved immunoprecipitation of endogenous complexes. Unfortunately, immunoprecipitation of septin subcomplexes using anti-SEPT2 antibody did not result in a coimmunoprecipitation of myosin II proteins, possibly due to steric inhibition, but immunoprecipitation of septin subcomplexes using anti-SEPT9 antibody, which coimmunoprecipitates SEPT2 (Surka et al., 2002) allowed coimmunoprecipitation of myosin II proteins (Figure 1E). Taken together, these data strongly support a bona fide SEPT2-Myosin II interaction in vivo.

SEPT2 Directly Binds to Amino Acids 1339-1630 of Myosin IIA

To test the possibility that SEPT2 and myosin II directly interact, we employed in vitro GST binding assays. Figure 2A is a schematic representation of myosin IIA and GST-fusions of the coiled-coil domain of myosin IIA (CCFL) as well as several truncations of this (CCT1-CCT5) that were generated are listed on Figure 2B. Since the tail domain is reported to be important for the dimerization/polymerization of myosin II (Ikebe et al., 2001), we reasoned that including this domain could make the recombinant proteins insoluble and/or cause an increase in nonspecific cosedimentation of soluble SEPT2 by

(B) Confocal images of isolated stress fibers stained with anti-SEPT2 antibody (green) and myosin II (green). F-actin was visualized by staining with rhodamine-phalloidin (red).
(C) Western blot of pull-downs of native myosin II using SEPT2/6/7 subcomplex immobilized on Ni-sepharose beads. 1% of the input and 33% of the pull-downs were loaded and the blots were probed with anti-myosin II antibody or anti-his antibody.
(D) Western blot of pull-downs of native SEPT2 using myosin II fragment (CCFL) immobilized on glutathione-sepharose beads. 1% of the input and 33% of the pull-downs were loaded and the blots were probed with anti-SEPT2 antibody or anti-GST antibody.
(E) Western blot of a SEPT9 immunoprecipitate probed with anti-myosin IIA antibody. 2% of the input and 10% of the immunoprecipitates were loaded. Bars represent 10 μm.

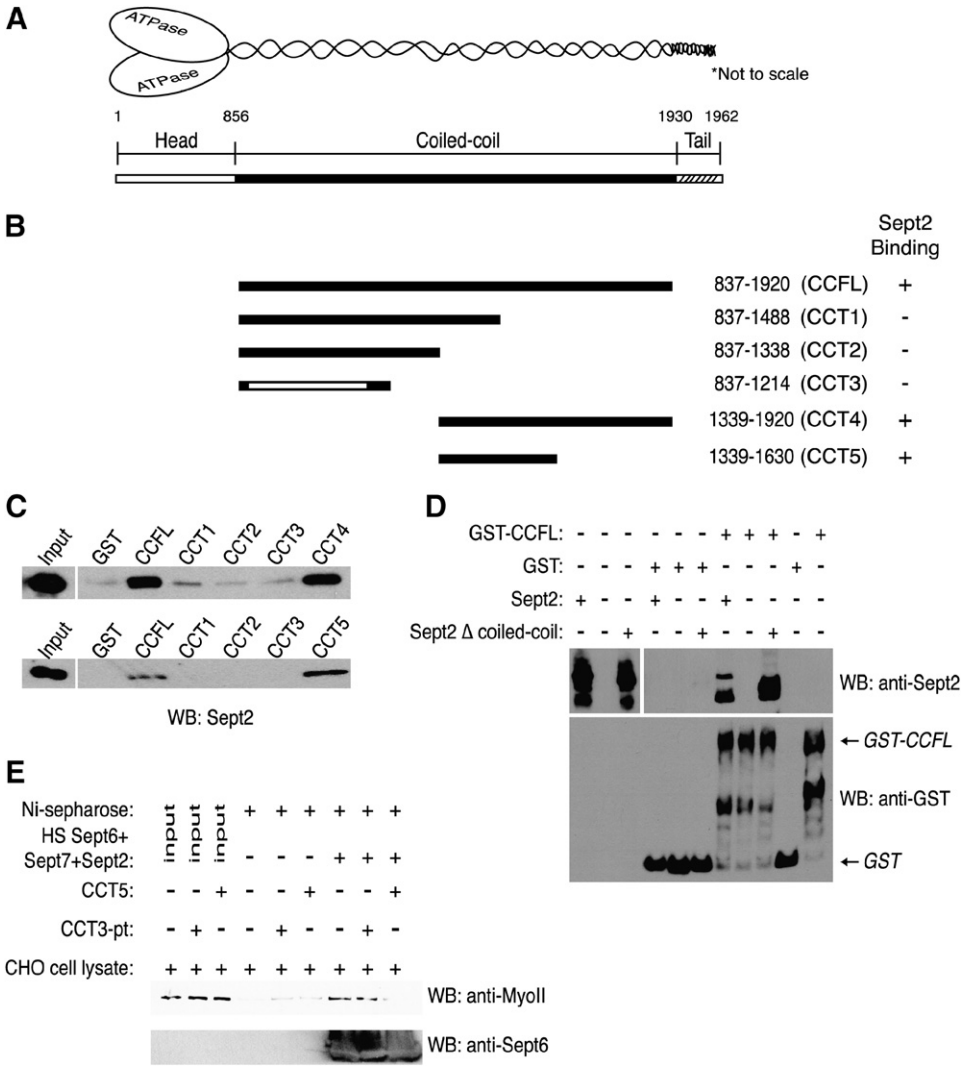

Figure 2. SEPT2 Directly Binds to Myosin IIA between Amino Acid 1339-1630

(A) Schematic diagram of myosin IIA showing the N-terminal head region that binds actin, the middle portion composed of coiled-coil region, and the C-terminal tail region, important for dimerization/polymerization of the heavy chain. Numbering of the amino acids indicate the approximate domain boundaries. Not to scale.

(B) Truncations of the coiled-coil domain of myosin IIA (CCFL, CCT1-CCT5) were tested for SEPT2 binding. All constructs generated for the binding study have N-terminal GST fusion tags. The relative ability of each construct to bind SEPT2 is summarized on the right. The indicated area of CCT3 (CCT3-pt) is used as a control.

(C) Representative western blots of pull-downs of soluble SEPT2 using the indicated truncation of the myosin coiled-coil domain immobilized on glutathione-agarose at a molar ratio of 2:1, respectively. 0.5% of the input and 50% of the pull-downs were loaded and the blots were probed with anti-SEPT2 antibody.

(D) Representative western blots showing in vitro pull-downs of soluble SEPT2 or SEPT2Δcoiled-coil and CCFL immobilized on glutathione-agarose beads at a molar ratio of 2:1, respectively. 1% of the input and 20% of the pull-downs were loaded and the blots were probed with anti-SEPT2 antibody.

(E) Representative western blot of Ni-sepharose pull-downs of native myosin II protein in the presence or absence of CCT5 or CCT3-pt. Peptides were added at a 10-fold molar excess. 0.5% of the input (lanes 1–3) and 100% of the pull-downs (lanes 4–9) were loaded and blots were probed with anti-myosin II antibody or anti-SEPT6 antibody.

trapping SEPT2 in myosin IIA polymers. Thus, the tail domain of myosin II (Figure 2A) was excluded from the binding studies. The GST-truncated myosin fusion constructs were purified and immobilized on glutathione-agarose or sepharose beads and their abilities to associate with soluble SEPT2 were assessed at a 2-fold molar excess of soluble SEPT2. As shown in Figure 2C, only CCFL and two truncations (CCT4 and CCT5) were able to pull down the soluble SEPT2 at levels above that of control beads and this interaction was saturable (Figure S1, see the Supplemental Data available with this article online). Three shorter fragments of myosin IIA corresponding to amino

acids 1339–1448, 1339–1435, and 1339–1532 were examined for their association to SEPT2, but their binding proved to be inconclusive (data not shown). The presence of the coiled-coil domains in septins and in the myosin tail raised the possibility that this interaction could be somewhat nonspecific. To address this possibility, we generated a soluble SEPT2 that lacks the coiled-coil region (SEPT2Δcoiled-coil) and found that it too was capable of binding CCFL (Figure 2D), indicating that the binding is not a coiled-coil interaction.

For further evidence that the binding is specific and that the CCT5 fragment is sufficient for binding, we asked whether this peptide could prevent the pull-down of myosin II from lysates on immobilized SEPT2/6/7 complexes. A 10-fold molar excess of soluble CCT5 or a similarly sized control peptide derived from amino acids 890 to 1190 of the coiled-coil domain of myosin IIA (CCT3-pt), shown in Figure 2B, were included in the pull-down of myosin II from cell lysates. As shown in Figure 2E, CCT5 successfully decreased the interaction of native myosin II molecules to septin subcomplexes, whereas CCT3-pt did not inhibit such association.

To determine if this peptide could disrupt the interaction of myosin and septins on actin filaments, we added CCT5 or the control CCT3-pt peptides to the isolated actin stress fibers. As shown in Figure 3A, CCT5 displaced SEPT2 from the isolated actin stress fibers, while the same concentration of CCT3-pt or GST (data not shown) had no effect. Although CCT5 caused dissociation of SEPT2, it did not affect the association of myosin II to the isolated actin stress fibers (Figure 3A, bottom row). Importantly, the disruption of SEPT2-myosin II binding was not observed when CCT5 was purified under denaturing conditions nor when the GST tag remained attached to the N-terminus of CCT5 (data not shown), indicating that the inhibitory effect of CCT5 required native folding conditions and removal of the bulky GST protein. Altogether, these data indicate that SEPT2 directly binds to myosin IIA and the minimum region on the myosin IIA required for the in vitro association to SEPT2 is amino acids 1339-1630.

CCT5 Disrupts the Typical Central Stress Fiber Localization of SEPT2

To examine the effects of SEPT2-myosin II dissociation in vivo, CCT5 or CCT3-pt was either overexpressed or transduced in CHO-K1 cells. Overexpression of CCT5, but not CCT3-pt, disrupted the filamentous appearance of SEPT2 (Figure 3B). In some cases, there appeared to be an overall decrease in SEPT2 levels in cells overexpressing CCT5; however, it is not clear whether this is due to an actual degradation of SEPT2 proteins or simply a decrease in fluorescence signals due to the disruption of SEPT2 filaments. Therefore, to more acutely inhibit the SEPT2-myosin II interaction, CCT5 and the control CCT3-pt were expressed as fusions with the TAT peptide (Schwarze et al., 2000). Similar disruption of SEPT2 filaments was observed in cells transduced with the TAT-CCT5 for 1.5 hr, but not when the control peptide (TAT-CCT3-pt) was added for the same duration (Figure 3C),

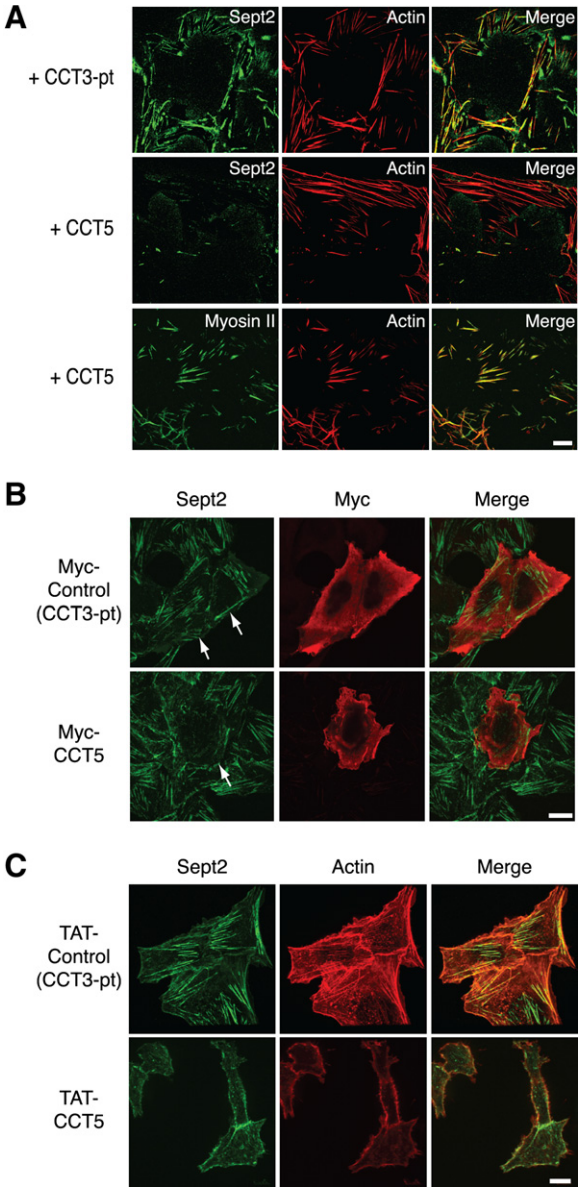

Figure 3. CCT5 Dissociates SEPT2 from Actin Stress Fibers

(A) Representative micrographs of isolated stress fibers from CHO-K1 cells exposed to CCT5 or CCT3-pt followed by immunostaining with antibodies against SEPT2 or myosin II (green). F-actin (red) was visualized by staining with rhodamine-conjugated phalloidin. 0.5μM of each protein was incubated with the isolated stress fibers.

(B) CCT5 and CCT3-pt were tagged with the myc epitope and transfected in CHO-K1 cells. These peptides were identified by immunostaining with anti-myc antibody (red) and endogenous SEPT2 was detected using anti-SEPT2 antibody (green).

(C) CHO-K1 cells were transduced with 1 μM of TAT-CCT5 or TAT-CCT3-pt for 1.5 hr. Endogenous SEPT2 was identified by using anti-SEPT2 antibody (green), and filamentous actin was visualized by staining with rhodamine conjugated phalloidin (red). Bars represent 10 μm.

and this occurred in virtually all cells in the culture. Furthermore, introduction of the TAT-CCT5 to CHO-K1 cells resulted in the loss of actin stress fibers and a significant

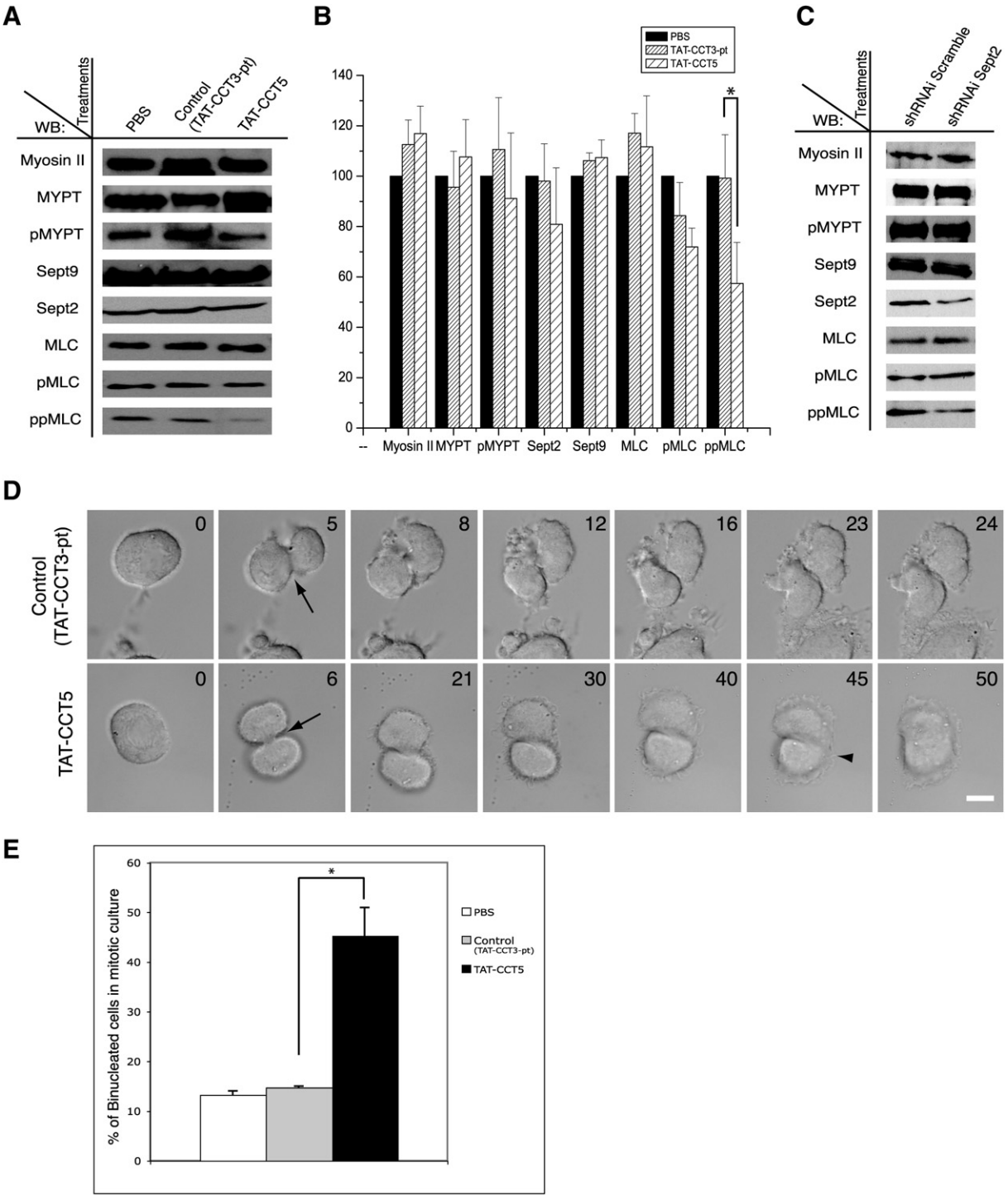

Figure 4. Dissociation of SEPT2 from Myosin II Alters Myosin II Activity and Increases the Number of Binucleated Cells

(A) Representative western blots of CHO-K1 whole-cell lysates prepared after incubating cells with PBS, the TAT-CCT3-pt, or TAT-CCT5 for 1.5 hr. Each lysate was probed with antibodies against the indicated proteins.

(B) Quantification of the western blots showing relative levels of myosin II, MYPT1, pMYPT1, SEPT2, SEPT9, MLC, pMLC, and ppMLC. Each experiment was done a minimum of three times, normalized to PBS transduction. The error bars reflect the standard deviation. *$p < 0.05$.

(C) Representative western blots of CHO-K1 whole-cell lysates prepared after transfecting with nonspecific shRNAi (shRNAi Scramble) or shRNAi silencing SEPT2. Each lysate was probed with antibodies against the indicated proteins.

(D) A representative recording of cell division shown over time depicting cells that were transduced with the TAT-CCT5 or TAT-CCT3-pt. Recordings were started at the beginning of karyokinesis. The number on each panel indicates the time elapsed from the starting point, expressed in minutes.

reduction in cell spreading. Thus, two different methods of introducing CCT5 resulted in disassembly of the SEPT2 filaments that normally localize on the central actin stress fibers.

Dissociation of SEPT2 from Myosin II Inhibits Myosin Activation and Function

The coincident disassembly of actin stress fibers with the disruption of the SEPT2-myosin II association by CCT5 suggested that the dissociation of SEPT2 from myosin II might alter the activity or the stability of myosin II, thereby affecting actin filament stability (Sellers, 1999). Therefore, to monitor the activity of myosin II, the levels of several myosin-associated proteins and their phosphorylation states were examined for changes after transduction with the inhibitory peptide (Figures 4A and 4B). pMLC-S19 and ppMLC-S19T18 levels were analyzed to determine the activation state of myosin II, MYPT1 phosphorylation (pMYPT1) was used as a measure of inactivation of MLC phosphatase by ROCK, and the levels of myosin II, SEPT2, and SEPT9 were assessed to determine if protein stabilities were affected by TAT-mediated transduction of the peptides (Figure 4A). Quantification of these proteins from at least three independent experiments showed a significant decrease in the levels of ppMLC-S19T18 ($p < 0.05$) (Figure 4B). None of the other proteins tested changed significantly after the disruption of SEPT2-myosin II interaction. A similar selective decrease in ppMLC-S19T18 was also observed when SEPT2 protein level was decreased with shRNAi (Figure 4C), a treatment previously shown to also disrupt actin stress fibers (Kinoshita et al., 2002), further supporting the notion that the CCT5 peptide affects only the SEPT2-myosin II interaction.

Since ppMLC-S19T18 is localized to the cleavage furrow and is proposed to play a role in cell division (Gerashchenko et al., 2002; Yamashiro et al., 2003), we arrested cells undergoing mitosis with nocodazole while treating with the TAT conjugated peptides for 1.5 hr prior to nocodazole washout. Indeed, we observed that cells transduced with CCT5 failed to complete cytokinesis whereas cells transduced with CCT3-pt divided normally (Figure 4D; see Movies S1 and S2). CHO-K1 cells treated with CCT5 began cytokinesis with normal initiation of the ingression of the cleavage furrow. Although the cleavage furrow appeared to have ingressed completely, the intercellular bridge subsequently relaxed and the cleavage furrow regressed rapidly, resulting in a binucleated cell (Figure 4D, lower panels). Often, as shown in this example, regression appeared to occur more rapidly at one side than the other, leading to unevenly shaped cells (Figure 4D panel 45′). Accordingly, there was a significant increase in the number of binucleated CHO-K1 cells transduced with CCT5, when compared to CCT3-pt (Figure 4E). In the mitotically enriched CHO-K1 cell cultures, 45.3% ± 5.6% of cells that had divided were binucleated ($n > 6$) when treated with CCT5 compared to 14.8 ± 1.0% ($n > 6$) and 13.3% ± 2.9% ($n > 6$) when transduced with the control peptide (CCT3-pt) or the vehicle PBS, respectively. It is not surprising that the furrow was able to ingress initially, since mono-phosphorylation of the MLC likely provided some contractile capacity, but the maintenance of the contracted midbody state appears to require di-phosphorylation (Mizutani et al., 2006).

CCT5 Dissociates Myosin IIA from SEPT2, CRIK, and ROCK

To visualize the localization of SEPT2 and myosin II in living cells, we stably transfected full-length myosin IIA tagged with td-Tomato into CHO-K1 cells that were already stably expressing inducible SEPT2-GFP. Stable clones expressing low levels of both proteins were selected for subsequent analyses. SEPT2 and myosin IIA localized to the cleavage furrow during cytokinesis as previously reported (Glotzer, 2001) (Figure 5A). Colocalization of these proteins became more evident as the ingression of the cleavage furrow progressed. SEPT2 and myosin IIA colocalized with each other for the duration of the experiment (Figure 5A).

We then examined their distribution upon TAT-CCT5 transduction. As shown in Figure 5B, initial ingression of the cleavage furrow progressed normally, comparable to the untreated cell, but the cleavage furrow subsequently regressed. Interestingly, myosin IIA no longer colocalized with SEPT2 (Figure 5C), which appeared to have remained in the cytoplasmic area where the furrow was previously constricted. This dissociation of the two proteins was more pronounced when photobleaching was minimized in fixed cells after the same treatments (Figure 5D). The SEPT2 signal can be seen spanning the gap between the opposed membranes, while myosin IIA appears to have regressed with the membrane. Furthermore, we observed that neither F-actin, as detected by phalloidin staining, nor plasma membrane, as detected by wheat germ agglutinin staining, was associated with the septins. The association of SEPT2 with myosin during early stages of mitosis may be mediated by anillin, an actin-, myosin-, and septin-binding protein released from the nucleus upon nuclear envelope breakdown. Indeed, at the stage when regression was observed, anillin was localized to the reforming nuclei (Figure 5E).

We wondered if the increase in binucleated cells caused by TAT-CCT5 was related to the decrease in ppMLC-S19T18. Three kinases, MLCK, ROCK, and citron kinase (CRIK), are known to play key roles in phosphorylating MLC and they are all important for cytokinesis (Matsumura,

Arrows indicate the ingressed furrow while the arrowhead highlights the asymmetric regression of the ingressed cleavage furrow. For a full QuickTime movie, refer to Movies S1 and S2.

(E) Quantification of binucleated cells transduced with the TAT-CCT5 or TAT-CCT3-pt. Minimum of 300 mitotic competent cells were counted. Mean values of binucleation of cells treated with PBS, TAT-CCT3-pt, and TAT-CCT5 were 13.29 ± 2.9, 14.78 ± 1.0, and 45.3 ± 5.6, respectively. Experiments were done a minimum of 3 times and the error bars represent the standard deviation. *$p < 0.05$.

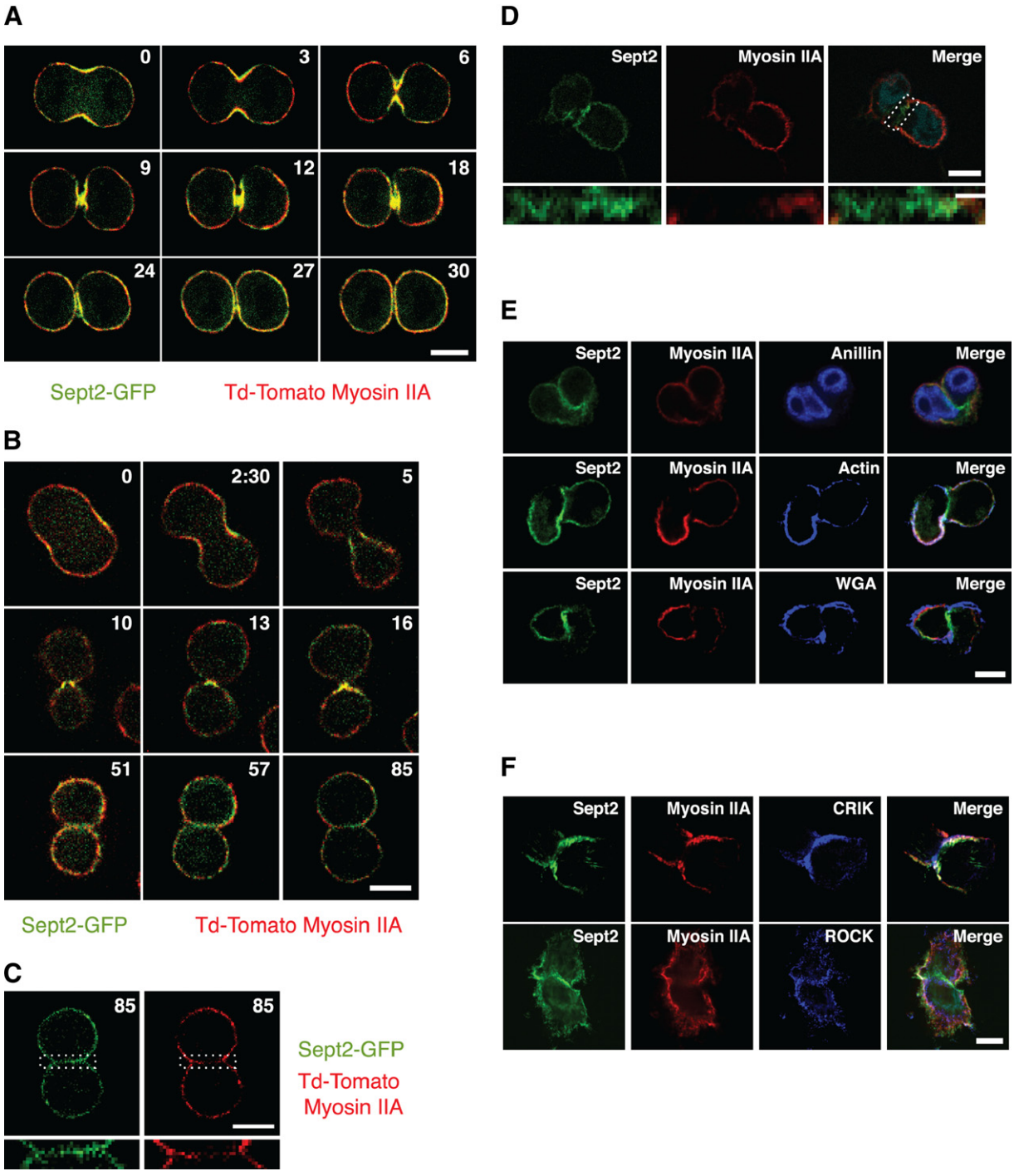

Figure 5. Myosin IIA Dissociates from SEPT2 and Myosin II Kinases during Cytokinesis

(A and B) CHO-K1 cell stably transfected with SEPT2-GFP and tdTomato-myosin IIA undergoing cytokinesis that is not treated (A) or transduced with TAT-CCT5 (B). A single confocal slice through the middle of the cell is shown. Numbers in each panel represent time elapsed in min from the starting point.

(C) Blow-up images of the last panel of part (B). The boxed area, what appears to be the center of the regressed cleavage furrow, is shown at a higher magnification.

(D) Confocal slice of a fixed mitotic CHO-K1 cell stably transfected with SEPT2-GFP (green) and tdTomato- myosin IIA (red) transduced with TAT-CCT5. DNA was visualized by staining with Hoechst (blue). The boxed area, depicting the cleavage furrow, is shown at a higher magnification.

(E) Representative CHO-K1 cells stably expressing SEPT2-GFP (green) and td-Tomato-myosin IIA (red) transduced with TAT-CCT5. The plasma membrane was visualized by staining with Alexa-fluor 633 conjugated wheat germ agglutinin (blue). F-actin was visualized by staining with Alexa-fluor 633 conjugated phalloidin (blue) and anillin was immunostained using anti-anillin antibody (blue).

2005). Therefore, we examined the distribution of CRIK and ROCK following TAT-CCT5-induced cleavage furrow regression. When stably transfected CHO-K1 cells were stained for CRIK or ROCK, we observed that a significant portion of these kinases were associated with SEPT2 at the center of regressed cleavage furrow (Figure 5F). Although we have been unable to document a SEPT2-kinase complex by immunoprecipitation (data not shown), the observed colocalization suggests that CRIK and ROCK may be associated with septins during the later stages of cytokinesis, and that septins may link these kinases to their substrate, myosin IIA, facilitating MLC phosphorylation and maintenance of the contractile ring.

Since dissociation of SEPT2 and myosin II proteins by inhibitory peptide CCT5 resulted in regression of myosin II and the membrane, while SEPT2, CRIK, and ROCK remained behind in the cytoplasm, we asked if this phenotype can be recapitulated by depleting SEPT2 proteins. As expected, the furrow also regressed when SEPT2 protein was knocked down with shRNAi and myosin II moved away from the center with the plasma membrane (Figure 6A, top panels). Moreover, when SEPT2 is knocked down with siRNA, the residual SEPT2 and CRIK remained predominantly in the cytoplasmic space between the regressed membranes (Figure 6A, bottom panels). In this case endogenous myosin II was detected using anti-myosin II antibodies, validating results obtained with the td-Tomato–myosin IIA reporter construct used in Figure 5.

Expression of Di-Phosphomimetic Myosin Light Chain, DD-MLC, Protects Cells from CCT5

The selective and specific decrease in the level of ppMLC-S19T18 upon CCT5 transduction implied that if the level of ppMLC-S19T18 were maintained, this should render cells resistant to CCT5. As predicted, cells expressing myc-tagged di-phosphomimetic MLC (myc-DD-MLC) but not mono-phosphomimetic MLC (myc-AD-MLC) or wild-type MLC (myc-WT-MLC) (Di Ciano-Oliveira et al., 2005; Iwasaki et al., 2001) showed resistance to CCT5-mediated loss of central stress fibers and alteration in cell morphology (Figure 6B), although the SEPT2 remained disrupted. Furthermore, cells transfected with myc-DD-MLC showed partial rescue from binucleation compared to the cells transfected with myc-WT-MLC or myc-AD-MLC (Figure 6C); 17.9% ± 2.70% cells that had divided where binucleated when transfected with DD-MLC compared to 25.73% ± 3.70% or 43.79% ± 3.28% when transfected with WT-MLC or AD-MLC, respectively. The observation of only partial rescue of cytokinesis was not surprising since cytokinesis likely requires both contraction of actomyosin structures and their disassembly (Yamashiro et al., 2003), the latter of which would be inhibited by the DD-MLC construct. Interestingly, expression of WT-MLC also shows a limited protection from the effects of the inhibitory CCT5 peptide, possibly due to the actions of endogenous kinases on overexpressed WT-MLC, which may increase the total amount of di-phosphorylated MLC. In contrast, AD-MLC, which cannot be di-phosphorylated, was unable to provide any rescue. In any case, the rescue by DD-MLC indicates that the only effect of CCT5 appears to be inhibition of MLC phosphorylation by displacing of SEPT2 from myosin II.

Inhibition of Myosin II Activation by CCT5 Is Preserved in Dividing Cells

Since nonsynchronized cell culture was used in Figure 4A and 4B, the selective decrease in the level of ppMLC-S19T18 upon CCT5 was mainly derived from interphase cells. We therefore asked if a similar decrease in ppMLC-S19T18 could be seen in dividing cells. When antibody specific for ppMLC-S19T18 was used to stain dividing cells that were treated either with CCT5 of CCT3-pt, there was an overall reduction in signal in the vicinity of the contractile ring in cells treated with CCT5 compared to the cells treated with CCT3-pt (Figure 7A). Interestingly, the poles of the cells did not show a decrease in the level of ppMLC-S19T18, suggesting that the effect is specific to regions where septins colocalize with myosin.

DISCUSSION

Our data indicate that SEPT2 associates with actin filaments by binding directly to myosin II. Immunofluorescence studies show that SEPT2 and myosin II isoform A (Figure 1A) and B (data not shown) colocalize even in the absence of filamentous actin. Anillin has been put forward as a putative adaptor protein, linking septins to the actin cytoskeleton (Kinoshita et al., 2002), and it appears to be a good candidate since it has actin and myosin II binding regions near the N terminus and a septin-interacting region near the C terminus (Kinoshita et al., 2002; Straight et al., 2005). However, anillin resides in the nucleus during interphase and becomes cytoplasmic only when the nuclear envelope breaks apart at the start of cell division (Oegema et al., 2000). Moreover, although anillin is necessary for recruitment of septin filaments to purified muscle actin bundles, there has been no direct interaction shown between anillin and septins and these two proteins have not been coprecipitated.

In contrast, our GST-binding studies indicate that SEPT2 interacts directly with a region of myosin IIA between amino acids 1339–1630, and this interaction is independent of the coiled-coil region of SEPT2. Addition of amino acids 1339–1630 of myosin IIA in pull-down experiments competed off native, full-length myosin II from the septin subcomplexes. Furthermore, the same peptide was able to dissociate SEPT2 from actomyosin filaments on isolated stress fibers. Antibody to SEPT9 (which coimmunoprecipitates SEPT2, Surka et al., 2002), was able to immunoprecipitate SEPT2 and myosin II together. Moreover, recombinant myosin II protein could pull down native septins and recombinant septin complexes could pull

(F) Representative CHO-K1 cells stably expressing SEPT2-GFP and td-Tomato-myosin IIA, transduced with TAT-CCT5 and immunostained with antibodies against CRIK or ROCK (blue). Bars represent 10 μm.

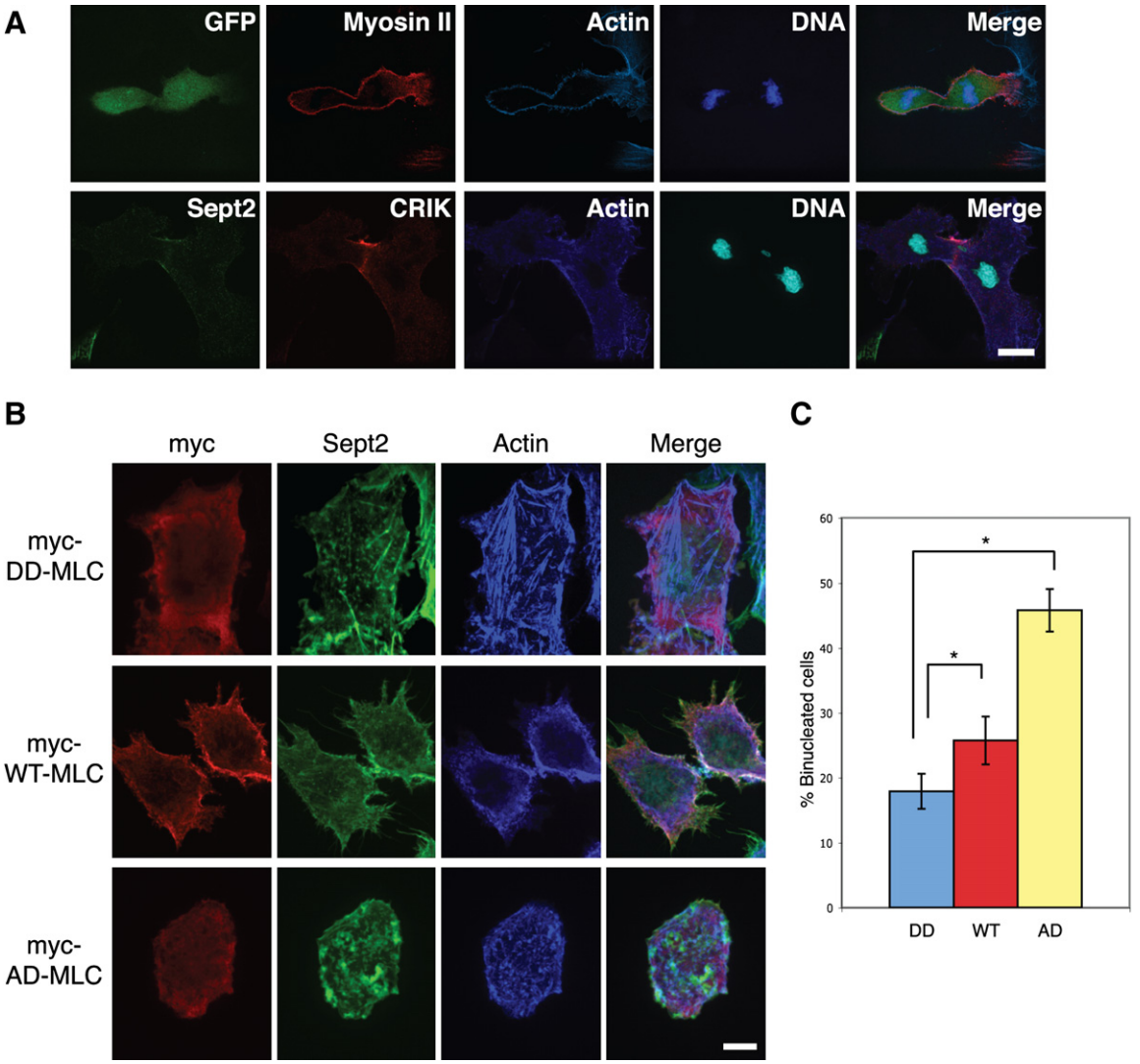

Figure 6. SEPT2 Knockdown Recapitulates the Loss of Myosin II and Transfection of DD-MLC Renders Cells Resistant to CCT5

(A) CHO-K1 cells transiently transfected with shRNAi SEPT2 (top panels) or siRNA SEPT2 (bottom panels). Transfected cells were identified by GFP or immunostaining with anti-SEPT2 antibody (green). Myosin II or CRIK was visualized by immunostaining with anti-myosin II antibody or anti-CRIK antibody, respectively (red). F-actin and DNA were visualized by staining with Alexa-fluor 633 conjugated phalloidin (blue) and Hoechst (teal), respectively.

(B) CHO-K1 cells were first transfected with myc-DD-MLC, myc-WT-MLC, or myc-AD-MLC, followed by TAT-CCT5 transduction. Transfected cells were identified by immunostaining with antibody specific for myc eptitope (red) and SEPT2 was visualized by immunostaining with anti-SEPT2 antibody (green). F-actin was visualized by staining with Alexa-fluor 633 conjugated phalloidin (blue).

(C) Quantification of binucleated cells transfected with different MLC constructs then transduced with TAT-CCT5. Minimum of 100 mitotic competent cells were counted in each experiment. Mean values of binucleation of cells transfected with myc-DD-MLC, myc-WT-MLC, and myc-AD-MLC, then transduced with TAT-CCT5 were 17.9% ± 2.7%, 25.3% ± 3.7% and 43.79% ± 3.28, respectively. Experiments were done 3 times and the error bars represent the standard deviation. *$p < 0.05$. Bars represent 10 μm.

down native myosin, suggesting that naturally occurring filamentous forms of the two proteins might interact in vivo. Taken together, our data indicate that SEPT2 directly binds to myosin IIA in vitro as well as in vivo (Figure 7B and C). This relationship may be evolutionarily conserved as previous yeast 2-hybrid studies have demonstrated a direct interaction between the *S. cerevisiae* type II myosin Myo1p and the sporulation-specific septin Spr3 (Drees et al., 2001).

Time-lapse fluorescence microscopy demonstrates that in dividing cells, SEPT2 colocalizes with myosin IIA at the cleavage furrow for the duration of ingression and stabilization of the midbody. By contrast, SEPT2 was dissociated from myosin IIA following the addition of the inhibitory peptide (CCT5), specifically at the last stages of cytokinesis where conspicuous segregation of these proteins was seen at the center of what appears to be the regressed cleavage furrow. The association of myosin and

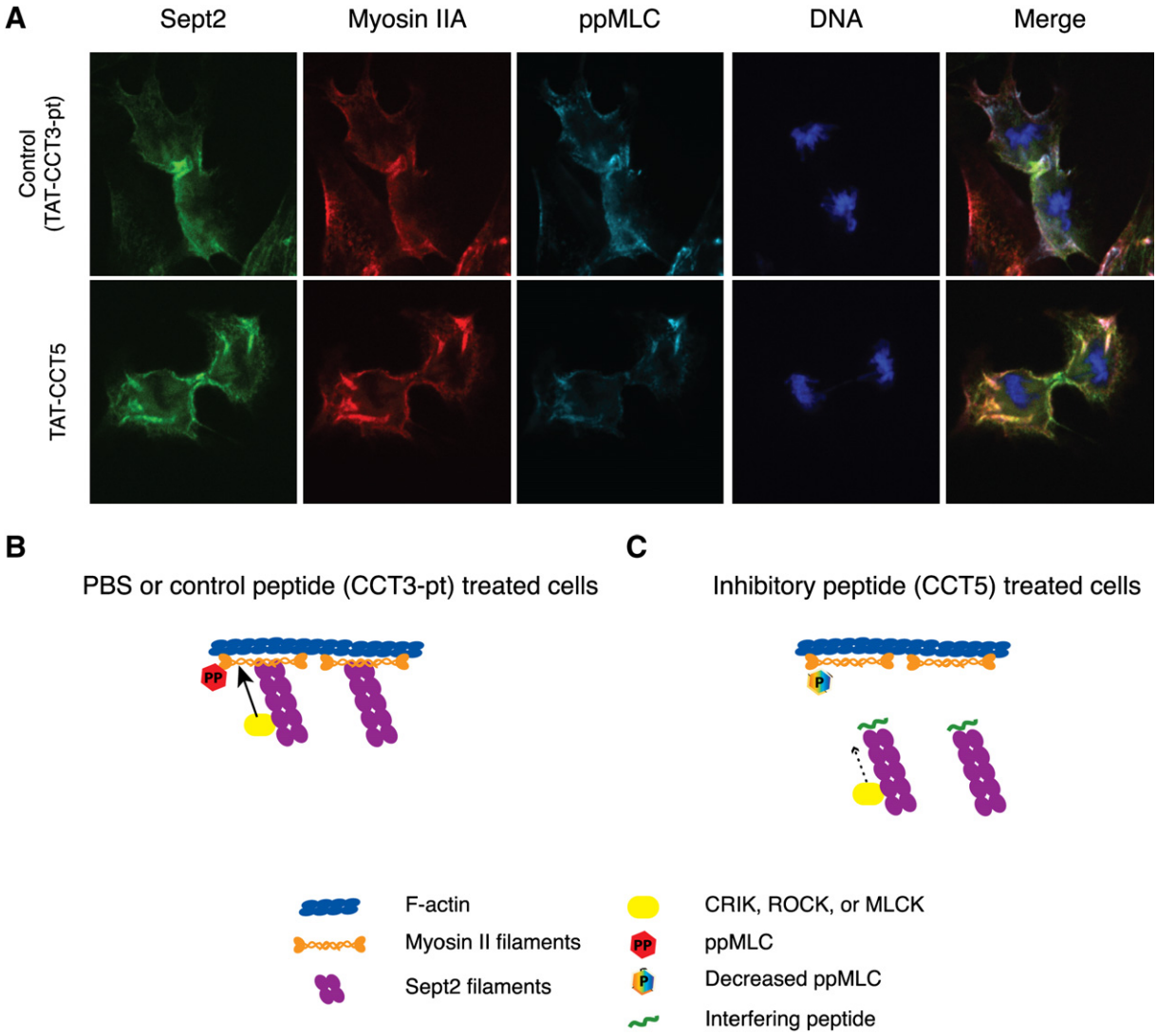

Figure 7. CCT5 Also Inhibits Myosin Activation in Dividing Cells

(A) Representative confocal micrographs of CHO-K1 cells stably expressing SEPT2-GFP (green) and td-Tomato-myosin IIA (red) that were transduced with TAT-CCT5 or TAT-CCT3-pt. ppMLC-S18T19 was visualized by immunostaining with anti-ppMLC-S18T19 antibody (teal). DNA was visualized by staining with Hoechst (blue). The same experimental conditions were applied in acquiring all of the images. Bar represents 10 μm.

(B and C) A model for SEPT2 as a molecular platform scaffolding myosin II and CRIK/ROCK to ensure a precise spatiotemporal activation of myosin II. During normal cell divisions the septin complex is localized to the cleavage furrow and provides a molecular platform for myosin II and CRIK/ROCK. This brings the enzyme and its substrate into close proximity, facilitating di-phosphorylation of myosin II, which in turn stabilizes the midbody and permits abscission to proceed. In the presence of the CCT5 peptide, the septins are displaced from myosin, inhibiting di-phosphorylation and destabilizing the midbody, resulting in regression of the cleavage furrow.

SEPT2 at early stages may be mediated by anillin, a protein which is capable of acting as an adaptor between septins and the actin cytoskeleton in vitro (Kinoshita et al., 2002). However, while anillin is present at the furrow during division, it enters the re-forming nuclei in late telophase. Thus, its function appears to be transient and perhaps important mainly for the initial recruitment of septins to the cleavage furrow. Similarly, in elegant immunofluorescence studies done by the Pollard group, anillin disappears from the cleavage furrow of *S. pombe* much earlier than septins, myosin, or actin (Wu et al., 2003).

Some septins associate with phospholipids (Casamayor and Snyder, 2003; Zhang et al., 1999). It was, therefore, surprising to observe that in the presence of CCT5, as the cleavage furrow regressed during aborted cytokinesis, the actomyosin ring retracted to the periphery of the plasma membrane while SEPT2 did not. Since hydrolysis of PIP_2 by PLC is required for the progression of cytokinesis (Wong et al., 2005), there may be a decrease in PIP_2 levels at the cleavage furrow during a specific stage of cytokinesis. The dissociation of SEPT2 from myosin II by TAT-CCT5 coupled with the disappearance of PIP_2 from

the cleavage furrow would limit the association of septin filaments with the plasma membrane, resulting in SEPT2 being left behind in the cytoplasm along the plane of division as the furrow regressed. More studies will be needed to determine the precise contribution of PIP_2 in anchoring septin filaments to the plasma membrane at the plane of division.

Although we were not able to document a direct interaction between SEPT2 and ROCK or CRIK, several lines of evidence suggest that SEPT2 can serve as a direct or indirect molecular platform for myosin II and ROCK or CRIK. First, both kinases have been reported to be responsible for generating ppMLC-S19T18 (Yamashiro et al., 2003), which is significantly decreased when the SEPT2-myosin II interaction is disrupted. In fact, expression of di-phosphomimetic MLC was able to rescue the cytokinesis defect in ROCK-depleted S2 cells (Dean and Spudich, 2006). Although expression of di-phosphomimetic MLC could not rescue the cytokinesis defect in citron-kinase-depleted S2 cells (Dean and Spudich, 2006), it did suppress the rough eye phenotype in *Drosophila* that is associated with depletion of citron kinase (D'Avino et al., 2004), suggesting that in some cases expression of di-phosphomimetic MLC can rescue citron-kinase-depletion phenotypes. Due to the partial redundancy between ROCK and CRIK, we were not able to test if the knockdown of either kinase phenocopies the effects of CCT5 peptide. Second, expression of di-phosphomimetic MLC (myc-DD-MLC) rendered cells resistant to the effects of CCT5 while expression of myc-AD-MLC did not, even though the latter should mimic pMLC-S19, supporting the notion that di-phosphorylation of MLC is critical and this is dependent on the SEPT2-myosin II interaction. Interestingly, expression of myc-WT-MLC resulted in a partial rescue from cytokinesis defects, presumably because even without a septin scaffold to facilitate kinase-substrate interactions, overexpression of this protein may allow enough protein to get phosphorylated by kinases such as ROCK. Third, when SEPT2 becomes displaced from the myosin II, CRIK and ROCK remain associated with it when myosin is absent. Finally, SEPT2 and the kinases may be indirectly linked by another protein such as polo-like kinase 1 (Plk1), for this protein has the ability to bind both to septins and the kinases (Lowery et al., 2007). Taken together, it appears that SEPT2 is a good candidate to form a molecular platform where myosin II kinases such as ROCK and CRIK can fully activate myosin II (i.e., ppMLC-S19T18), and this di-phosphorylation is needed for the completion of cytokinesis.

CCT5 transduction disrupted actin stress fibers and inhibited cytokinesis. An intricate relationship between septins and actin has been suggested by others (Kinoshita et al., 2002; Schmidt and Nichols, 2004), where actin directs the stability of septins. However, consistent with the previously published data, it does not appear that this relationship is unidirectional—that is, that actin fibers are solely supporting septin filaments. Rather, it seems that septins are capable of governing the actin fibers by regulating the activity of myosin II, an actin bundling protein that stabilizes F-actin. A number of lines of evidence suggest that CCT5 specifically affects the association of SEPT2 to myosin II without affecting other functions. First, CCT5 specifically and selectively dissociates SEPT2 from the actomyosin filaments on the isolated stress fibers. Second, the function of myosin does not seem to have been generally altered by this peptide since myosin remains attached to the isolated stress fibers and, more importantly, the initial ingression of the cleavage furrow occurs normally. Third, ROCK activity does not appear to be disrupted by CCT5 as evidenced by the normal levels of pMYPT1. Fourth, exogenous expression of DD-MLC was able to render cells resistant to CCT5, suggesting that maintaining the level of ppMLC-S18T19 was sufficient to alleviate the effects of disrupting SEPT2-myosin II interaction. Lastly, a partial knockdown of SEPT2 by shRNAi or siRNA phenocopies the effects seen with CCT5 transduction. Taken together, CCT5 appears to specifically affect the association of SEPT2 and myosin II.

It is interesting that di-phosphorylation of myosin light chain is particularly sensitive to the septin-myosin interaction, and that this level of myosin activation appears necessary for the maintenance, although not the initial contraction, of the contractile ring. Di-phosphorylation of MLC has been seen in a variety of other cellular contexts and it will be of interest to determine the roles played by septins in modulating other processes such as cell migration, membrane fusion, and morphogenesis.

EXPERIMENTAL PROCEDURES

cDNA Constructs and Transfections

pEGFP-TRE nonmuscle myosin heavy chain IIA (myosin IIA) was a gift from R. Adelstein (National Institute of Health, Bethesda, MD). pTAT-HA was a gift from S. Dowdy (University of California, San Diego, CA). pRSET-tdTomato was a gift from R. Tsien (University of California, San Diego, CA). p15A-PT7-SEPT2 and pET30a-HS-SEPT6+SEPT7(NT) were gifts from I. Macara (Virginia University School of Medicine, Charlottesville, VA). Myc-pcDNA3.1+ was a gift from R. Collins (The Hospital for Sick Children, Toronto, ON). pcDNA3.1 myc-DD-MLC, pcDNA3.1 myc-AD-MLC, and pcDNA3.1 myc-WT-MLC were gift from C. Di Ciano-Oliveira (University of Toronto, Toronto, ON). The SEPT2 gene targeting sequence previously published (Kinoshita et al., 2002) was synthesized for siRNA (Dharmacon) or cloned into psiRNA3-hH1GFPzeoG2 (InvivoGen) for hairpin shRNA expression.

Myosin IIA fragments, CCFL (aa 837–1920), CCT1 (aa 837–1488), CCT2 (aa 837–1338), CCT3 (aa 837–1214), CCT4 (aa 1339–1920), CCT5 (aa 1339–1630), and CCT3-pt (aa 890–1190) were produced by PCR amplification and cloned into pTAT-HA, myc-pcDNA3.1+, pGEX6p (Invitrogen) and/or pQE-30 (QIAGEN). pZeo-tdTomato was generated by PCR amplification of tdTomato from pRSET-tdTomato then subcloning into the Nhe1-HindIII sites of pZeocin (Invitrogen). Full-length myosin IIA was subcloned into the HindIII and SpeI sites of pZeo-tdTomato. Three rounds of subcloning were done in order to generate pTRE2hyg-SEPT2-GFP. First, SEPT2 cDNA from pGEX-2T-SEPT2 (Xie et al., 1999) was subcloned into the pcDNA3.1+ (Invitrogen), which was then subcloned into the pEGFP-N1 (Clontech) (pEGFP-N1-SEPT2). DNA region encoding SEPT2 and GFP from pEGFP-N1-SEPT2 was then subcloned into the NotI and BglII sites of pTRE2hyg (Clontech). SEPT2 lacking coiled-coil region, SEPT2Δ coiled-coil (aa 1-301), was produced by PCR amplification and cloned into pGEX-KG (GE Healthcare).

All transfections of plasmids were performed with FuGENE6 (Roche) or Lipofectamine 2000 (Invitrogen) according to the manufacturers'

instructions. For transient transfection, cells were assayed 12–72 hr posttransfection. For stable transfections, cells were exposed to 1 mg/ml Hygromycin (Sigma) or 0.5 μg/ml Zeocin (Invitrogen) 2 d post-transfection to select for the stably transfected cells.

Protein-Protein Interaction Studies

Myosin IIA fragments were purified using glutathione-agarose or glutathione-sepharose beads according to the manufactures' guidelines (Sigma or GE Healthcare) in lysis buffer A (30 mM Tris-Cl [pH 7.5], 50 mM KCl, 1 mM $MgCl_2$, 1 mM $CaCl_2$, 2 mM EDTA, 2 mM EGTA, 1 mM DTT, and protease inhibitors). Recombinant SEPT2 or SEPT2Δ coiled-coil was generated using lysis buffer B (50 mM Tris-Cl [pH 8.0], 100 mM NaCl, 20% glycerol, 5 mM $MgCl_2$, 10 mM EDTA, 0.05% tween-20, 40μM GDP, 1 mM DTT, and protease inhibitors). GST was cleaved with thrombin (Sigma). Binding studies were performed as described (Beites et al., 1999) using binding buffer (buffer A supplemented with 0.05% tween-20, 0.2% BSA, 0.2% gelatin, 0.2% Nonidet P-40, and 0.5% Triton X-100). SEPT2 elution buffer volume was kept to less than 5%. Beads were washed 4–5 times in binding buffer without protease inhibitors.

Myosin II pull-downs were performed similar to in vitro binding studies as described (Beites et al., 1999) where SEPT2/6/7 subcomplex was isolated as described (Sheffield et al., 2003) and CHO-K1 cell lysates were made either in buffer C (50 mM MOPS [pH 7.0], 0.1 mM EGTA, 0.1% Tx-100, 1 mM ATP, 0.1M NaCl, 1% 2-mecaptoethanol, and protease inhibitors) or buffer D (50 mM Tris-Cl [pH 8.0], 50 mM NaCl, 0.5% Tx-100, 0.05% tw-20, 2 mM EDTA, 2 mM EGTA, 1 mM DTT, and protease inhibitors).

Immunoprecipitation was performed as described in (Surka et al., 2002), and probed for myosin IIA (1:1000, Covance).

Microscopy

CHO-K1 cells were fixed with 2%–4% paraformaldehyde (Electron Microscopy) and processed for immunostaining as described previously in (Birukova et al., 2004; Xie et al., 1999). The fixed cells were stained for SEPT2 (1:1000; Xie et al., 1999), myosin II (1:200; Biomedical Technologies), anillin (1:5000 serum), ppMLC-S18T19 (1:100 Cell Signaling), CRIK (1:200; BD Biosciences), and/or ROCK II (1:200; Upstate Biotechnology). Anti-anillin antibody was generated in a rabbit exactly as described in Oegema et al. (2000). F-actin was visualized with phalloidin coupled to rhodamine, Alexa 488 or 633 (1:200; Invitrogen). Plasma membrane was visualized with wheat germ agglutinin coupled to Alexa 633 (1:200; Invitrogen). Images were acquired using PlanApo 63x/1.4 (oil) objective on a spinning disk confocal microscope (AX70 Provis; Leica) with a cooled charge-coupled device camera (DP70; Hammasuto) using Volocity software (Improvision).

CHO-K1 cells were exposed to 1.25 μM aphidicoline (Sigma) for 14–16 hr then incubated with 50 nM nocodazole (Sigma) and 1 μM of TAT peptides for 1.5 hr in fresh AMEM. This was followed by incubation with another fresh AMEM containing only nocodazole for an additional 3 hr. To wash out nocodazole, treated cells were washed four times with an excess amount of fresh AMEM.

Live cell division was visualized on a temperature-controlled stage (37°C) of a Leica DMIRE2 inverted microscope using the DIC filter with 63× oil objective. Recordings were made at 1 m intervals by acquiring images digitally using a cooled charge-coupled device camera (Hamamatsu Photonics, Japan) controlled by Openlab software (Improvision). Recorded images were exported as .tiff files and QuickTime movies.

Stress Fiber Isolation and Peptide-Mediated Dissociation

Stress fibers were isolated as described in (Katoh et al., 1998) strictly abiding to a brief extraction with 0.5% Triton X-100 containing HEPES (pH 7.2) for maximum of 3 min on ice.

For dissociation of SEPT2 from myosin on stress fibers, GST-tagged recombinant peptides encoding amino acids 1339-1630 or 890-1190 of the myosin IIA were purified as described above. Peptides from which GST was removed were added to the isolated stress fiber for 1 hr in 50 mM Tris-Cl, 75 mM KCl, 3 mM $MgCl_2$, 1 mM $CaCl_2$, 1 mM EGTA, and 20 mM imidazole (pH 7.2) on ice. For competition pull-down assays, similarly generated peptides were added at a 10-fold excess in buffer C.

For TAT transduction-mediated dissociation of SEPT2 from myosin II, TAT conjugated peptides were generated as described in (Becker-Hapak et al., 2001) with minor modifications; bacterial cells were lysed in a French pressure cell and the purified peptides were dialyzed against PBS.

CHO-K1 cells were transduced with 1 μM of TAT peptides for 1.5 hr then processed for imaging, fixing, or collecting samples.

Collected samples were probed for SEPT9 (1:1000; Surka et al., 2002), SEPT2 (1:1000), myosin II (1:1000), MYPT1 or pMYPT1 (1:1000; Upstate Biotechnology), and pMLC or ppMLC (1:1000; Cell Signaling Technology). The intensity of each band from nonsaturating exposures was converted to a numerical value using the ImageJ program. After subtracting background, each band was compared to those from PBS treated cells. For statistical analyses, student's t tests were done and values are reported as the mean ± SD.

Supplemental Data

The Supplemental Data include one figure and two movies and can be found with this article online at http://www.developmentalcell.com/cgi/content/full/13/5/677/DC1/.

ACKNOWLEDGMENTS

We thank Drs. R. Adelstein, S. Dowdy, R. Tsien, I. Macara, C. Di Ciano-Oliveira, Y. Huang, and Mr. R. Collins for reagents, the Imaging Facility at the Hospital for Sick Children (M. Woodside and P. Paroutis), Vilte Barakauskas for technical assistance early in the project, Dr. C. Froese for editorial assistance, Dr. G. Boulianne for comments on the manuscript, and all members of the Trimble Lab for discussions and advice. W.S.T. is the recipient of the Canada Research Chair in Molecular Cell Biology and this work was supported by the Canadian Cancer Society.

Received: November 17, 2006
Revised: June 24, 2007
Accepted: September 7, 2007
Published: November 5, 2007

REFERENCES

Barral, Y., Mermall, V., Mooseker, M.S., and Snyder, M. (2000). Compartmentalization of the cell cortex by septins is required for maintenance of cell polarity in yeast. Mol. Cell *5*, 841–851.

Becker-Hapak, M., McAllister, S.S., and Dowdy, S.F. (2001). TAT-mediated protein transduction into mammalian cells. Methods *24*, 247–256.

Beites, C.L., Xie, H., Bowser, R., and Trimble, W.S. (1999). The septin CDCrel-1 binds syntaxin and inhibits exocytosis. Nat. Neurosci. *2*, 434–439.

Berlin, A., Paoletti, A., and Chang, F. (2003). Mid2p stabilizes septin rings during cytokinesis in fission yeast. J. Cell Biol. *160*, 1083–1092.

Birukova, A.A., Smurova, K., Birukov, K.G., Usatyuk, P., Liu, F., Kaibuchi, K., Ricks-Cord, A., Natarajan, V., Alieva, I., Garcia, J.G., et al. (2004). Microtubule disassembly induces cytoskeletal remodeling and lung vascular barrier dysfunction: role of Rho-dependent mechanisms. J. Cell. Physiol. *201*, 55–70.

Casamayor, A., and Snyder, M. (2003). Molecular dissection of a yeast septin: distinct domains are required for septin interaction, localization, and function. Mol. Cell. Biol. *23*, 2762–2777.

Castillon, G.A., Adames, N.R., Rosello, C.H., Seidel, H.S., Longtine, M.S., Cooper, J.A., and Heil-Chapdelaine, R.A. (2003). Septins have a dual role in controlling mitotic exit in budding yeast. Curr. Biol. *13*, 654–658.

D'Avino, P.P., Savoian, M.S., and Glover, D.M. (2004). Mutations in sticky lead to defective organization of the contractile ring during cytokinesis and are enhanced by Rho and suppressed by Rac. J. Cell Biol. *166*, 61–71.

Dean, S.O., and Spudich, J.A. (2006). Rho kinase's role in myosin recruitment to the equatorial cortex of mitotic Drosophila S2 cells is for myosin regulatory light chain phosphorylation. PLoS ONE *1*, e131.

Di Ciano-Oliveira, C., Lodyga, M., Fan, L., Szaszi, K., Hosoya, H., Rotstein, O.D., and Kapus, A. (2005). Is myosin light-chain phosphorylation a regulatory signal for the osmotic activation of the Na+-K+-2Cl-cotransporter? Am. J. Physiol. Cell Physiol. *289*, C68–C81.

Drees, B.L., Sundin, B., Brazeau, E., Caviston, J.P., Chen, G.C., Guo, W., Kozminski, K.G., Lau, M.W., Moskow, J.J., Tong, A., et al. (2001). A protein interaction map for cell polarity development. J. Cell Biol. *154*, 549–571.

Fujiwara, T., Bandi, M., Nitta, M., Ivanova, E.V., Bronson, R.T., and Pellman, D. (2005). Cytokinesis failure generating tetraploids promotes tumorigenesis in p53-null cells. Nature *437*, 1043–1047.

Gerashchenko, B.I., Ueda, K., Hino, M., and Hosoya, H. (2002). Phosphorylation at threonine-18 in addition to phosphorylation at serine-19 on myosin-II regulatory light chain is a mitosis-specific event. Cytometry *47*, 150–157.

Glotzer, M. (2001). Animal cell cytokinesis. Annu. Rev. Cell Dev. Biol. *17*, 351–386.

Hanrahan, J., and Snyder, M. (2003). Cytoskeletal activation of a checkpoint kinase. Mol. Cell *12*, 663–673.

Hartwell, L.H. (1971). Genetic control of the cell division cycle in yeast. IV. Genes controlling bud emergence and cytokinesis. Exp. Cell Res. *69*, 265–276.

Ikebe, M., and Hartshorne, D.J. (1985). Phosphorylation of smooth muscle myosin at two distinct sites by myosin light chain kinase. J. Biol. Chem. *260*, 10027–10031.

Ikebe, M., Komatsu, S., Woodhead, J.L., Mabuchi, K., Ikebe, R., Saito, J., Craig, R., and Higashihara, M. (2001). The tip of the coiled-coil rod determines the filament formation of smooth muscle and nonmuscle myosin. J. Biol. Chem. *276*, 30293–30300.

Iwasaki, T., Murata-Hori, M., Ishitobi, S., and Hosoya, H. (2001). Diphosphorylated MRLC is required for organization of stress fibers in interphase cells and the contractile ring in dividing cells. Cell Struct. Funct. *26*, 677–683.

Joberty, G., Perlungher, R.R., Sheffield, P.J., Kinoshita, M., Noda, M., Haystead, T., and Macara, I.G. (2001). Borg proteins control septin organization and are negatively regulated by Cdc42. Nat. Cell Biol. *3*, 861–866.

Joo, E., Tsang, C.W., and Trimble, W.S. (2005). Septins: traffic control at the cytokinesis intersection. Traffic *6*, 626–634.

Katoh, K., Kano, Y., Masuda, M., Onishi, H., and Fujiwara, K. (1998). Isolation and contraction of the stress fiber. Mol. Biol. Cell *9*, 1919–1938.

Kinoshita, M., Kumar, S., Mizoguchi, A., Ide, C., Kinoshita, A., Haraguchi, T., Hiraoka, Y., and Noda, M. (1997). Nedd5, a mammalian septin, is a novel cytoskeletal component interacting with actin-based structures. Genes Dev. *11*, 1535–1547.

Kinoshita, M., Field, C.M., Coughlin, M.L., Straight, A.F., and Mitchison, T.J. (2002). Self- and actin-templated assembly of Mammalian septins. Dev. Cell *3*, 791–802.

Kusch, J., Meyer, A., Snyder, M.P., and Barral, Y. (2002). Microtubule capture by the cleavage apparatus is required for proper spindle positioning in yeast. Genes Dev. *16*, 1627–1639.

Lowery, D.M., Clauser, K.R., Hjerrild, M., Lim, D., Alexander, J., Kishi, K., Ong, S.E., Gammeltoft, S., Carr, S.A., and Yaffe, M.B. (2007). Proteomic screen defines the Polo-box domain interactome and identifies Rock2 as a Plk1 substrate. EMBO J. *26*, 2262–2273.

Matsumura, F. (2005). Regulation of myosin II during cytokinesis in higher eukaryotes. Trends Cell Biol. *15*, 371–377.

Mizutani, T., Haga, H., Koyama, Y., Takahashi, M., and Kawabata, K. (2006). Diphosphorylation of the myosin regulatory light chain enhances the tension acting on stress fibers in fibroblasts. J. Cell. Physiol. *209*, 726–731.

Nguyen, T.Q., Sawa, H., Okano, H., and White, J.G. (2000). The *C. elegans* septin genes, unc-59 and unc-61, are required for normal postembryonic cytokineses and morphogenesis but have no essential function in embryogenesis. J. Cell Sci. *113*, 3825–3837.

Oegema, K., Savoian, M.S., Mitchison, T.J., and Field, C.M. (2000). Functional analysis of a human homologue of the *Drosophila* actin binding protein anillin suggests a role in cytokinesis. J. Cell Biol. *150*, 539–552.

Schmidt, K., and Nichols, B.J. (2004). Functional interdependence between septin and actin cytoskeleton. BMC Cell Biol. *5*, 43.

Schwarze, S.R., Hruska, K.A., and Dowdy, S.F. (2000). Protein transduction: unrestricted delivery into all cells? Trends Cell Biol. *10*, 290–295.

Sellers, J.R. (1999). Myosins, Second Edition (Oxford, New York: Oxford University Press).

Sheffield, P.J., Oliver, C.J., Kremer, B.E., Sheng, S., Shao, Z., and Macara, I.G. (2003). Borg/septin interactions and the assembly of mammalian septin heterodimers, trimers, and filaments. J. Biol. Chem. *278*, 3483–3488.

Straight, A.F., Field, C.M., and Mitchison, T.J. (2005). Anillin binds nonmuscle myosin II and regulates the contractile ring. Mol. Biol. Cell *16*, 193–201.

Surka, M.C., Tsang, C.W., and Trimble, W.S. (2002). The mammalian septin MSF localizes with microtubules and is required for completion of cytokinesis. Mol. Biol. Cell *13*, 3532–3545.

Takizawa, P.A., DeRisi, J.L., Wilhelm, J.E., and Vale, R.D. (2000). Plasma membrane compartmentalization in yeast by messenger RNA transport and a septin diffusion barrier. Science *290*, 341–344.

Tasto, J.J., Morrell, J.L., and Gould, K.L. (2003). An anillin homologue, Mid2p, acts during fission yeast cytokinesis to organize the septin ring and promote cell separation. J. Cell Biol. *160*, 1093–1103.

Versele, M., Gullbrand, B., Shulewitz, M.J., Cid, V.J., Bahmanyar, S., Chen, R.E., Barth, P., Alber, T., and Thorner, J. (2004). Protein-protein interactions governing septin heteropentamer assembly and septin filament organization in *Saccharomyces cerevisiae*. Mol. Biol. Cell *15*, 4568–4583.

Wong, R., Hadjiyanni, I., Wei, H.C., Polevoy, G., McBride, R., Sem, K.P., and Brill, J.A. (2005). PIP2 hydrolysis and calcium release are required for cytokinesis in Drosophila spermatocytes. Curr. Biol. *15*, 1401–1406.

Wu, J.Q., Kuhn, J.R., Kovar, D.R., and Pollard, T.D. (2003). Spatial and temporal pathway for assembly and constriction of the contractile ring in fission yeast cytokinesis. Dev. Cell *5*, 723–734.

Xie, H., Surka, M., Howard, J., and Trimble, W.S. (1999). Characterization of the mammalian septin H5: distinct patterns of cytoskeletal and membrane association from other septin proteins. Cell Motil. Cytoskeleton *43*, 52–62.

Xue, J., Tsang, C.W., Gai, W.P., Malladi, C.S., Trimble, W.S., Rostas, J.A., and Robinson, P.J. (2004). Septin 3 (G-septin) is a developmentally regulated phosphoprotein enriched in presynaptic nerve terminals. J. Neurochem. *91*, 579–590.

Yamashiro, S., Totsukawa, G., Yamakita, Y., Sasaki, Y., Madaule, P., Ishizaki, T., Narumiya, S., and Matsumura, F. (2003). Citron kinase, a Rho-dependent kinase, induces di-phosphorylation of regulatory light chain of myosin II. Mol. Biol. Cell *14*, 1745–1756.

Zhang, J., Kong, C., Xie, H., McPherson, P.S., Grinstein, S., and Trimble, W.S. (1999). Phosphatidylinositol polyphosphate binding to the mammalian septin H5 is modulated by GTP. Curr. Biol. *9*, 1458–1467.